ELSEVIER

Polymer 44 (2003) 481–493

polymer

www.elsevier.com/locate/polymer

Phase continuity and inversion in polystyrene/poly(methyl methacrylate) blends

C.Z. Chuai[a,b,*,1], K. Almdal[c], J. Lyngaae-Jørgensen[b]

[a]*Department of Chemical Engineering, Tianjin Institute of Light Industry, 1038 Dagunan Road, 300222 Tianjin, People's Republic of China*
[b]*Danish Polymer Centre, Building 423, Technical University of Denmark, DK-2800 Kgs. Lyngby, Denmark*
[c]*Danish Polymer Centre, Risø National Laboratory, P.O. Box 49, DK-4000 Roskilde, Denmark*

Abstract

Dual-phase continuity and phase inversion of polystyrene (PS)/poly(methyl methacrylate) (PMMA) blends processed in a twin-screw extruder was investigated using a selective extraction technique and scanning electron microscopy. Emphasis was placed on investigating the effects of viscosity ratio, blend composition, processing variables (mixing time and annealing) and diblock copolymer addition on the formation of bi-continuous phase structure (BPS) in PS/PMMA blends. The experimental results were compared with the volume fraction of phase inversion calculated with various semi-empirical models. The results showed that the formation of a BPS strongly depends on the blend composition and the viscosity ratio of the constituent components. Furthermore, BPS was found in a wide volume fraction interval. Increasing the mixing time and the addition of diblock copolymer, both led to a narrowing range of volume fraction in which BPS exists. Quiescent annealing coarsened the structure but indicated no qualitative changes. Some model predictions for phase inversion could predict qualitative aspects of the observed windows of co-continuity but none of the models could account quantitatively for the observed data.

Keywords: Polystyrene; Poly(methyl methacrylate); Polymer blends

1. Introduction

Blending of two or more thermoplastics may generate new materials with a combination of properties not found in the pure polymers. Blending is often a faster and more cost-effective way of achieving the required properties than synthesizing new polymers. The property of a polymer critically depends on its morphology. Therefore, understanding blend morphology development during processing and the influence of blend morphology on material properties can greatly aid the tailoring of polymer blends.

Polymer blends may or may not be miscible, depending on the specific interactions between polymer chains. However, most polymers are immiscible and produce multiphase blends. These blends combine characteristics of both constituent polymers in a manner that is intimately related to the blend morphology, (i.e. the shape and the size of the dispersed phase particles). The morphology of the blend on a micro-scale develops during melt processing in a very complex way. Phenomena like deformation, break-up and/or coalescence of the dispersed phase particles can occur when a multiphase system is submitted to a field of flow. Under the appropriate conditions morphological structures such as spheres, ellipsoids, fibres and plates or ribbons can be produced.

The morphology of immiscible polymer blends shows a remarkable diversity but fundamentally a distinction between (a) blends with discrete phase structure (DPS) and (b) blends with co-continuous or bi-continuous phase structure (BPS) can be made. In two-phase blends with BPS both components form phases that partly or fully form a continuous phase which mutually interpenetrate each other and permeate through the whole sample volume [1]. The transition from DPS to BPS is fundamental in the sense that BPS in principle represents an infinite structure for an infinitely large sample. The influence of viscosity ratio, phase viscoelasticity, normal stresses, interfacial tension, blend composition, flow type and relevant relationships in such structures have been extensively studied during the last decade [1–5]. Structure development in classical processing equipment such as internal mixers or extruders has received

* Corresponding author. Address: Room 102, Door 12, Xiao Hai Di Rongjiang Li, Tianjin 300222, People's Republic of China. Tel.: +86-22-2834-2736.
E-mail address: chengzhichuai@hotmail.com (C.Z. Chuai).
[1] Present address: Danish Polymer Centre, Building 423, Technical University of Denmark, DK-2800 Kgs. Lyngby, Denmark. Tel.: +45-4525-6808; fax: +45-4588-2161.

0032-3861/03/$ - see front matter © 2002 Elsevier Science Ltd. All rights reserved.
PII: S0032-3861(02)00632-8

particular attention [6–16]. However, due to the lack of control of the flow conditions and the inability to make a direct observation of the blending process, only qualitative relations between structure and processing conditions have so far been proposed. Moreover, several aspects of the dispersion process and the coalescence phenomena remain to be elucidated.

Many papers have considered the so-called phase inversion phenomenon and its prediction. The term originates from observations of behaviour of Newtonian liquid mixtures like oil in water. For such low viscosity mixtures one observes discrete drops of oil in water when the system is sheared with low volume fractions of oil. By increasing the oil volume fraction a system inversion occurs at a critical volume fraction when the system changes to water drops in a continuous oil phase. At the critical phase inversion volume fraction and eventually in a narrow volume fraction interval a BPS may be observed. Some authors [15,17–22] have previously suggested that phase inversion occurs at a particular melt composition. Other authors [16,23–28] have explained that phase inversion is primarily a coalescence phenomenon.

The point of phase inversion, at which co-continuity is observed, can be related to the rheology of the pure materials through semi-empirical models [29–31]. The early semi-empirical model that the phase inversion was determined by a relationship between the torque ratio and the composition (volume fraction) was formulated by Avgeropoulos et al. [32] expressed as:

$$\frac{T_1}{T_2} = \frac{\varphi_{1I}}{\varphi_{2I}} \tag{1}$$

where T_i is the torque of pure component i at the blending conditions and φ_{iI} is the volume fraction of component i, here $\varphi_{1I} = 1 - \varphi_{2I}$.

For blends prepared at low shear rates, Paul and Barlow [30] proposed a similar theoretical prediction of the phase inversion and viscosity ratio. Other researchers [29,31] later expressed this semi-empirical equation as

$$\frac{\eta(\dot{\gamma})_1}{\eta(\dot{\gamma})_2} = \frac{\varphi_{1I}}{\varphi_{2I}} \equiv \lambda, \qquad \text{or} \qquad \varphi_{2I} = 1/(1+\lambda) \tag{2}$$

where η_i is the viscosity of component i at the shear rate of blending and φ_{iI} is the volume fraction of component i. The validity of this equation was corroborated and developed further by several authors [29,31,33,34] for blends with a viscosity ratio close to unity. For example, Jordhamo et al. [29], based on the volume fraction and viscosity, developed the following rheological viscosity–volume fraction expressions:

$$\frac{\eta_1}{\eta_2}\frac{\phi_{2I}}{\phi_{1I}} \begin{cases} \geq 1 & \text{phase 2 continuous} \\ \leq 1 & \text{phase 1 continuous} \\ \cong 1 & \text{dual phase continuity} \end{cases} \tag{3}$$

where phase 2 is continuous when the left hand side is greater than unity, phase 1 is continuous when the quantity is less than unity, and dual-phase continuity arises when the quantity is approximately unity.

Based on the filament instability concept, Metelkin and Blekht [35] derived another model to predict critical volume fraction for phase inversion as

$$\varphi_{2I} = \frac{1}{1+\lambda F(\lambda)} \tag{4}$$

where $F(\lambda) = 1 + 2.25 \log \lambda + 1.81(\log \lambda)^2$.

Utracki [36] suggested a model that can be used to predict the point of phase inversion for blends with a viscosity ratio away from unity

$$\lambda = \frac{\eta_1}{\eta_2} = \left[\frac{(\varphi_m - \varphi_{2I})}{(\varphi_m - \varphi_{1I})}\right]^{[\eta]\varphi_m} \tag{5}$$

where $[\eta]$ is the intrinsic viscosity of the dispersed phase and φ_m is the maximum packing volume fraction. This model predicts that phase inversion concentration is bound by the limits of the maximum packing volume fraction, related to the onset of the co-continuity of phases. For most polymer blends (spherical domains), the maximum packing volume fraction in Eq. (5) can be taken as $\varphi_m = 1 - \varphi_{cr}$, where φ_{cr} is the critical volume fraction for percolation [37]. The theoretical value of φ_{cr} is equal to 0.156 (thus, $\varphi_m = 0.844$) and the optimum value of the intrinsic viscosity $[\eta]$ is 1.9 [36]. The present models of viscosity ratio (Eqs. (2), (4) and (5)) for phase inversion in mechanical blends are limited to low shear rates (viscosity ratios).

Control of blend parameters can be a very complex task. As the commercial importance of polymer blends increases, a more rigorous understanding of morphology control during processing will be required. A practical way of stabilizing blend morphologies is by modifying the interface between the two components. This can be achieved by addition of block copolymers comprising blocks partially compatible with the individual polymers [38]. Another method of modifying the interface is by reactive extrusion in which grafts are formed between the reactive sites of the blend components [39]. In the presence of interfacial modifiers, it is possible to obtain blends with both co-continuous structures and improved mechanical properties.

Many investigators [8,10,15,29,33,39–47] have reported on BPS in immiscible polymers. Interpenetrating polymer blends or polymer blends with BPS are known to possess relatively stable morphologies [48,49]. Identifying the mechanism that controls how co-continuity develops is a key step in mastering the processing-morphology relationship.

In this study, we used a Haake twin-screw extruder to investigate the phase structure of polystyrene (PS) and poly(methyl methacrylate) (PMMA) blends. The phase structure of the polymer blends was identified using scanning electron microscopy (SEM). For the study we

Table 1
Characteristics and sources of the raw materials

Sample code	$\bar{M}_w$ [a] (kg/mol)	$\bar{M}_n$ [a] (kg/mol)	$\bar{M}_z$ [a] (kg/mol)	$\bar{M}_w/\bar{M}_n$	Density[b] (kg/m^3)	Grade and source
PS_1	329.1	133.1	534.6	2.47	1030	N7000, Shell
PS_2	207.6	90.8	358.8	2.29	1030	Polystyol 144C, BASF
PMMA	79.3	43.7	121.1	1.80	1188	Plexiglass 7N, Rohm and Haas
PS-*b*-PMMA	170.9	162.4	178.2	1.05	–	P719-SMMA, Polymer Source, Inc.

The PS-*b*-PMMA diblock copolymer was symmetrical, 50:50 wt%.
[a] Measured at DTU laboratory by SEC instrument and the standard deviation on the molar mass was ±3%.
[b] Derived from Ref. [51] at 20 °C.

prepared PS/PMMA binary blends with and without diblock copolymer (PS-*b*-PMMA) using a selective extraction technique [1,8,10] to observe the phase structure and to determine the degree of co-continuity of the given blends. A selective extraction technique provides a 'gentle' treatment of the sample and, by this means, one of the blend components may be removed from the system while the other retains the phase structure that it exhibited within the blend. This phase may then be examined directly with SEM. Entire morphologies of the phase structure can be examined, not just a two-dimensional slice or a fracture surface. This allows for observation of complex morphology structures because the large depth of field of SEM enables observation of the whole sample surface area.

The primary objectives of the present study were (1) to determine the viscosity ratio of the constituent components and the composition under which a co-continuous phase structure may be formed, (2) to compare the effect of mixing time and PS-*b*-PMMA diblock copolymer on the phase structure and composition range of dual-phase continuity, (3) to investigate whether or not a co-continuity phase structure, if formed, is stable from different mixing stages, and (4) to determine phase inversion in PS/PMMA blends experimentally and to compare the results with theoretical predictions.

2. Experimental

2.1. Materials

The characteristics and commercial sources of the polystyrene (PS), poly(methyl methacrylate) (PMMA) and PS-*b*-PMMA diblock copolymer used in this study are shown in Table 1. Using blends of these polymers we investigated morphology evolution during melt blending in a Haake twin-screw extruder.

2.2. Mixing equipment, torque measurements and experimental procedures

Blends were prepared using a 5/14 mm diameter conical twin-screw extruder (Haake MiniLab Rheomex CTW5). This extruder can be used in two ways, extrusion (flush) or cycle blends (as shown schematically in Fig. 1). The screw length was 109.5 mm and the diameter of the one-hole circular flush die was 2 mm. The screw configuration employed had one 30 mm length kneading block. The temperatures of the extruder were set at 200 °C in each zone (flush die, cycle flow channel, and barrel zones) and a screw speed of 30 rpm was used for all blends. A torque trace was recorded for each blending run. The equilibrium torque

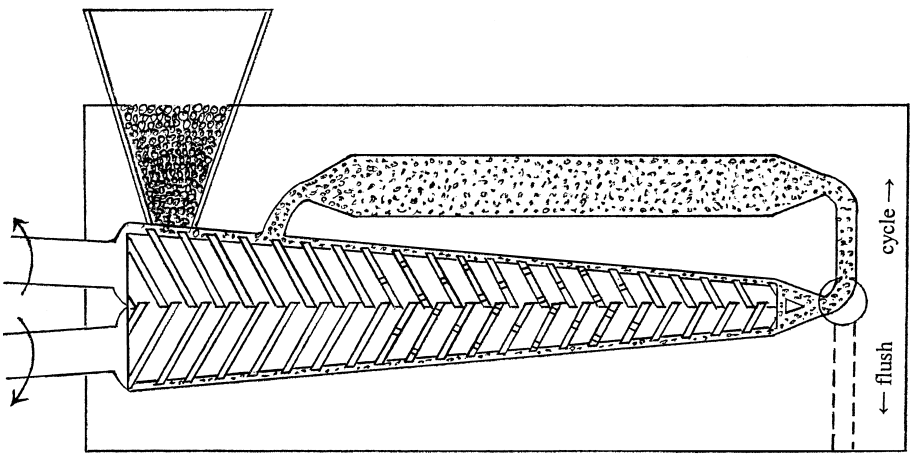

Fig. 1. Schematic diagram describing a conical twin-screw extruder, in which a pair of immiscible polymers are extruded under a preset temperature profile along the extruder axis.

Table 2
Torque, viscosity and density values of the raw materials

Sample code	Torque[a] (Nm)	Viscosity[b] (Pa s) at $\dot{\gamma} = 117\ s^{-1}$	Density[c] (kg/m^3) at 200 °C
PS_1 (N7000), Shell	32	700	972
PS_2 (144C), BASF	17	350	972
PMMA (7 N), Rohm and Haas	42	2404	1097

[a] Measured at DTU laboratory using Haake MiniLab Rheomex CTW5 twin-screw extruder for 10 min mixing.
[b] Measured at DTU laboratory using Rosand precision capillary extrusion rheometer.
[c] Derived from Ref. [51].

values, obtained after the set mixing time, and the densities of the polymers at 200 °C of the polymers are given in Table 2. The torque values (10 min mixing) were used to calculate the volume fractions of the blends for phase inversion.

Before a typical experiment the PS and the PMMA polymers in pellets were dried at 60–65 °C under vacuum for a week to remove moisture. In all experiments a total of 6 g mixtures of PS and PMMA, with or without a PS-*b*-PMMA diblock copolymer, was weighed according to the density of each polymer at 200 °C. The blend was manually premixed by rolling the given blend ratio in a bag for about 10 min before being fed into the hopper of the extruder. A nitrogen blanket was used to minimize polymer degradation. Mixing time was counted from the time when the materials were loaded into the extruder. Typically, 30–40 s were required to load the material. In preparing the samples we varied blend composition and the duration of melt blending.

2.3. Size exclusion chromatography

Molar masses for PS, PMMA and PS/PMMA blends with and without the diblock copolymer were measured by size exclusion chromatography (SEC) at 25 °C in tetrahydrofuran (THF) before and after hot stage run. As expected no significant changes (less than 3%) in molar mass were observed as a result of polymer blending.

2.4. Rheological measurements

A Rosand Precision Capillary Extrusion Rheometer (Rosand Model RH-7, Rosand Precision Limited) with a capillary rheometer of 1 mm, a length-to-diameter ratio of 16 and an entrance angle of 180° was used to measure the viscosities of the polymers at high shear rates (1–10,000 s^{-1}). The Bagley end correction and Rabinowitsch correction were applied in calculating the wall shear stress. The viscosity values of each polymer are given in Table 2.

2.5. Annealing

Annealing tests were carried out at 200 °C. The samples were placed in a mould using a hydraulic laboratory moulding press (USA CARVER, model 3851CE). The samples were then cooled down rapidly by cooling water on the sample kept within the circle holes of the mould to freeze the morphology. All the samples were annealed for 28 min at the set temperature.

2.6. Scanning electron microscopy

The fractured surface of the extrudates was prepared by cryogenic fracturing in liquid nitrogen. In order to aid in identification the fracture surface, some samples before coating were selectively extracted with solvents to remove certain components. All sample surfaces were sputter coated with a 25 nm layer of gold before examination. The morphology of the cross-section of extrudates was examined by SEM in JEOL Model JSM-840 and JSM-5900 microscopes at 14, 15 or 20 kV accelerating voltages.

2.7. Selective extraction technique

The samples of PS/PMMA blends with and without diblock copolymer were extruded at set processing conditions. The samples were fractured at liquid nitrogen temperature and then heated with selective solvents at 40 °C for 10 days. Cyclohexane and formic acid were used as selective solvents for PS and PMMA, respectively. After extracting the samples were dried at 60 °C under vacuum for two weeks. The extraction and drying cycle were repeated several times until a constant weight of remaining polymer was obtained. The purpose of the selective extraction was to determine the degree of continuity and to aid in identifying SEM morphology for both PS and PMMA.

The degree of continuity of a phase can be defined as the fraction of the polymer, which can be selectively extracted by a solvent expressed as [1]

$$\text{Degree of continuity } (\varphi_{i,\text{con}}) = \frac{\text{extracted mass of component } i}{\text{mass of component } i \text{ before extraction}} \quad (6)$$

where $\varphi_{i,\text{con}}$ is the degree of continuity of phase i. The plot of $\varphi_{i,\text{con}}$ as a function of the volume fraction of component i in the blend, φ_i, provides a continuity map of the blend. From the continuity maps the critical volume fraction for onset of forming continuous structures of phase i, $\varphi_{\text{cr},i}$, can

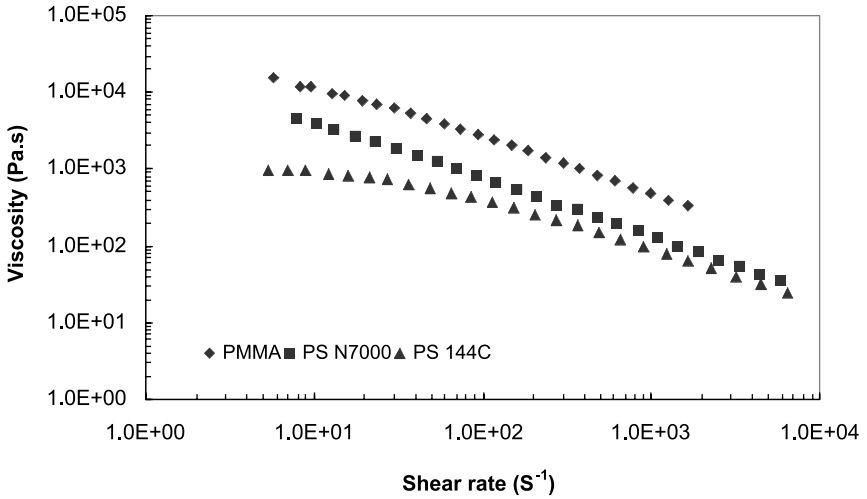

Fig. 2. Viscosity as a function of shear rate at 200 °C for PS and PMMA from capillary rheometry.

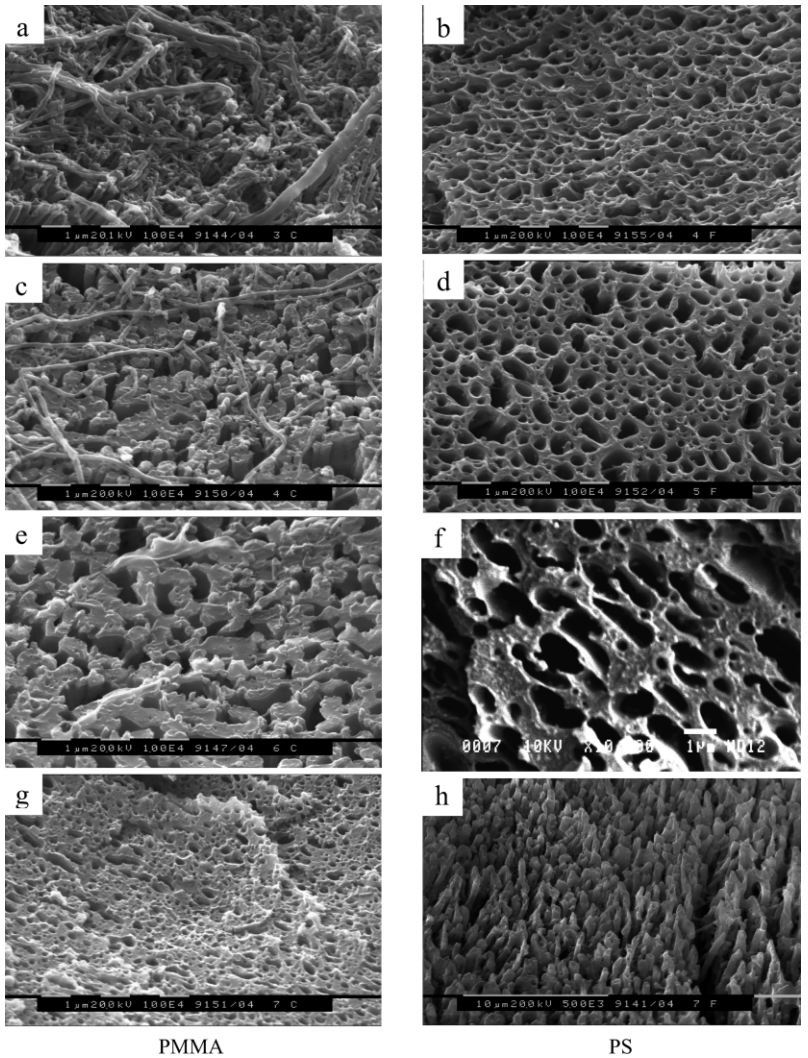

Fig. 3. SEM images of the PMMA phase after PS extraction and the PS phase after PMMA extraction in 10 min mixed PS_1/PMMA blends: (a) and (b) $\varphi_{PMMA} = 0.30$; (c) and (d) $\varphi_{PMMA} = 0.40$; (e) and (f) $\varphi_{PMMA} = 0.60$; (g) and (h) $\varphi_{PMMA} = 0.75$.

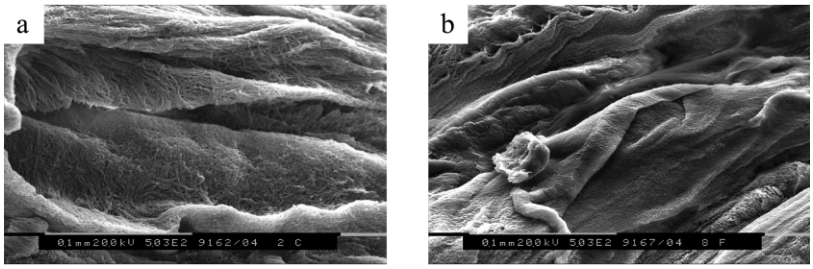

Fig. 4. SEM images of the PMMA phase after PS extraction and the PS phase after PMMA extraction in PS_1/PMMA blends for 10 min mixing: (a) $\varphi_{PMMA} = 0.20$; (b) $\varphi_{PMMA} = 0.85$.

be estimated. $\varphi_{cr,i}$ is the value of φ_i at which $\varphi_{i,con}$ becomes non-zero.

3. Results and discussion

3.1. Influence of composition and viscosity ratio

In order to investigate the influence of the viscosity ratio, λ, the samples were prepared at two different values of λ. The viscosity of the components, PMMA, PS_1 (N7000) and PS_2 (144C), were measured at 200 °C for $\dot{\gamma} = 1 - 10{,}000\ s^{-1}$ by using a capillary rheometer (Fig. 2). The viscosity of PMMA is much higher than that of PS_1 and PS_2 over the entire range of shear rates tested and the viscosity of PS_1 is higher than that of PS_2, especially at low $\dot{\gamma}$. At low shear rate, the viscosity of PS_2 seems to have a Newtonian plateau-like behaviour.

Blends of PMMA with PS_1 and PS_2, respectively, were prepared by mixing for 10 min. The phase structures are characterized through SEM images after selective extractions and the interval of BPS determined from plots of $\varphi_{PS,con}$ and $\varphi_{PMMA,con}$ as a function of the φ_{PMMA}. For the PS_1/PMMA blends SEM images are presented in Figs. 3 and 4 and the so-called continuity mapping in Fig. 5. For the PS_2/PMMA blends SEM images are presented in Fig. 6 and the continuity map in Fig. 7. In the 10 min mixed PS_1/PMMA system a BPS is observed in all four blends in the range $0.30 \leq \varphi_{PMMA} \leq 0.75$ irrespective of whether the PS_1 or PMMA phase has been extracted indicating phase co-continuity in this volume fraction interval. Furthermore, the micrographs of PMMA and PS_1 at the same φ_{PMMA} match quite well. The PMMA phase of the $\varphi_{PMMA} = 0.20$ sample and the PS phase of the $\varphi_{PMMA} = 0.85$ sample were spongy and collapsed during extraction, but remained one coherent structure (Fig. 4). However, the PMMA phase of the $\varphi_{PMMA} = 0.10$ sample (extracted PS phase) and the PS phase of the $\varphi_{PMMA} = 0.90$ samples (extracted PMMA phase) collapsed to a powder during extraction and no SEM images were obtained. The maximum error in the estimation of $\varphi_{cr,i}$ (the critical volume fraction for the onset of forming continuous structures of phase i) is estimated to be less than $\pm 5\%$ from the spongy samples. Thus, we estimate that $\varphi_{cr,PMMA} = 0.20 \pm 0.05$ and $\varphi_{cr,PS} = 0.15 \pm 0.05$ in PS_1/PMMA blends system. It is interesting to observe (Fig. 3(a) and (h)) that the minority phase in the co-continuous blends are stretched out into fibrillar-like structures. Determination of the critical volume fraction from Fig. 5 by extrapolation of degree of continuity versus φ_{PMMA} curves yields $\varphi_{cr,PMMA} = 0.21$ and $\varphi_{cr,PS} = 0.16$.

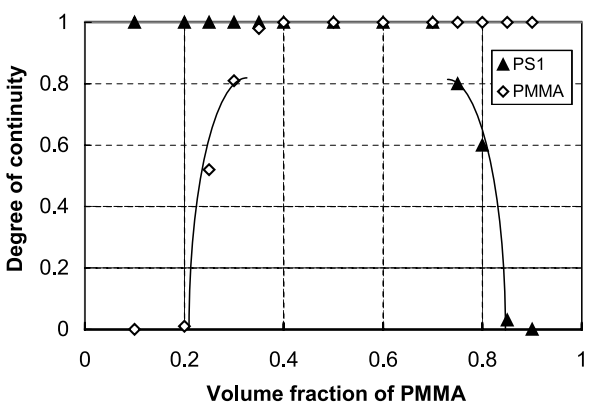

Fig. 5. Degree of continuity as a function of volume fraction of PMMA for PS_1/PMMA blends at 200 °C, 10 min mixing.

The critical volume fraction (φ_{cr}) can be estimated either as the volume fraction where the minor phase polymer collapses and disintegrates after extraction of the major phase resin or by extrapolation of the continuity index curve to zero. In general, the results of these two methods should coincide. A difference may point to erroneous results, e.g. by structure breakdown caused by the swelling pressure of the absorbed solvent, or by stress cracking of the separating walls between domains [1]. In this study, the critical volume fractions (φ_{cr}) determined by these two methods are in excellent agreement.

In the 10 min mixed PS_2/PMMA system a co-continuous structure is observed in all four blends (Fig. 6) in the range $0.40 \leq \varphi_{PMMA} \leq 0.80$ irrespective of whether the PS_2 or PMMA phase has been extracted indicating phase co-continuity in this composition interval. Furthermore, the micrographs of PMMA and PS_2 at the same φ_{PMMA} match quite well. It is interesting to note that the $\varphi_{PMMA} = 0.40$ shows a coalescent morphology of PMMA droplets (Fig. 6(a)). The PMMA phase of the $\varphi_{PMMA} = 0.30$ sample and

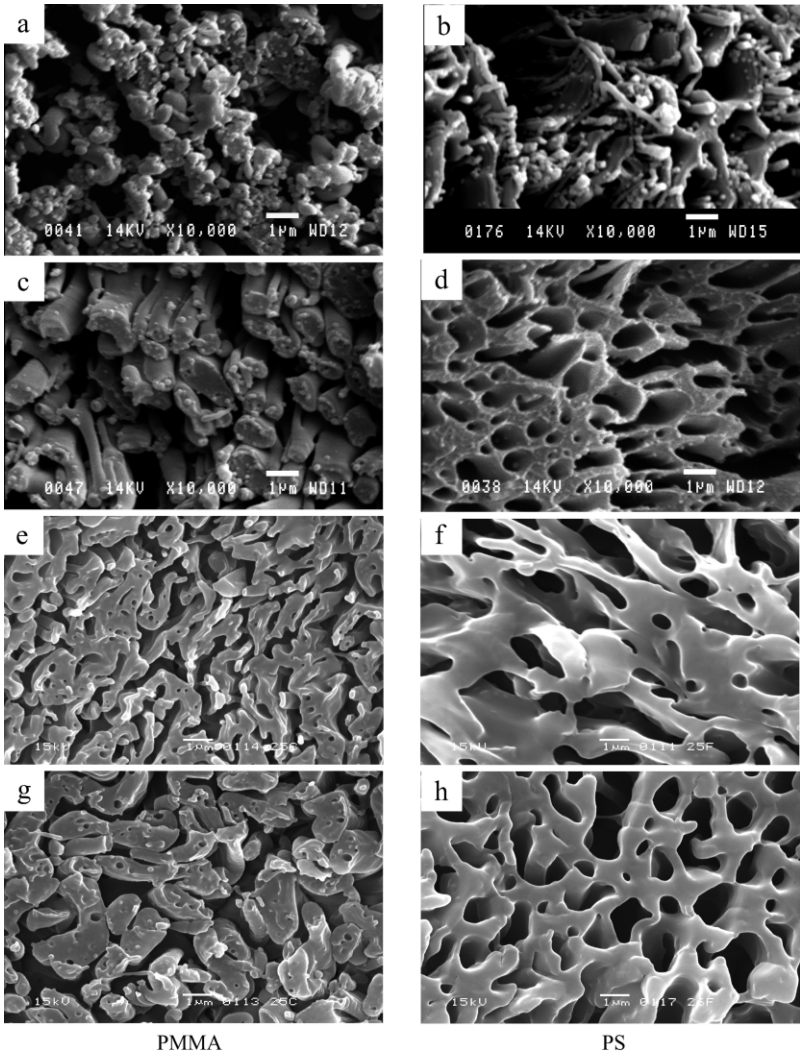

Fig. 6. SEM images of the PMMA phase after PS extraction and the PS phase after PMMA extraction in PS_2/PMMA blends for 10 min mixing: (a) and (b) $\varphi_{PMMA} = 0.40$; (c) and (d) $\varphi_{PMMA} = 0.60$; (e) and (f) $\varphi_{PMMA} = 0.70$; (g) and (h) $\varphi_{PMMA} = 0.80$.

the PS $\varphi_{PMMA} = 0.85$ sample were spongy and collapsed during extraction, but remained as one coherent structure (not shown). The PMMA phase of the $\varphi_{PMMA} = 0.20$ sample and the PS phase of the $\varphi_{PMMA} = 0.90$ sample disintegrated to powders during extraction. We estimate that $\varphi_{cr,PMMA} = 0.30 \pm 0.05$ and $\varphi_{cr,PS} = 0.15 \pm 0.05$ in PS_2/PMMA blends system. Determination of the critical volume fraction from Fig. 7 by extrapolation of the degree of continuity as a function of φ_{PMMA} curves yields $\varphi_{cr,PMMA} = 0.30$ and $\varphi_{cr,PS} = 0.17$, respectively, in good agreement with the assessments from the micrographs.

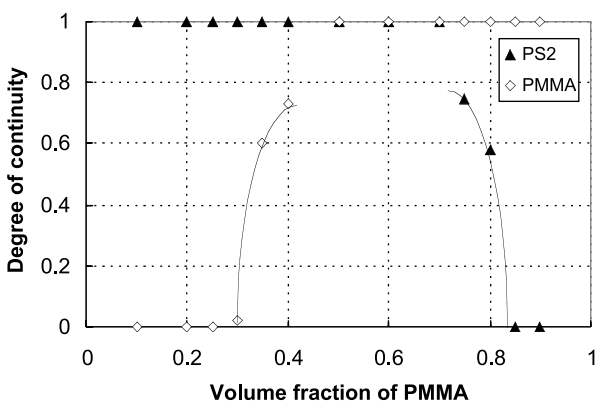

Fig. 7. Degree of continuity as a function of volume fraction of PMMA for PS_2/PMMA blends at 200 °C, 10 min mixing.

A comparison of the $\varphi_{cr,i}$ values in the PS_1/PMMA (Figs. 3–5) and PS_2/PMMA (Figs. 6 and 7) systems indicates that the polymer with lower viscosity (the polystyrenes) has a lower value of $\varphi_{cr,i}$. An asymmetric—with respect to $\varphi_{PMMA} = 0.50$—BPS interval for the existence of co-continuous structures exist in both the systems.

3.2. Influences of mixing time

The PS_2/PMMA system was used to investigate the effect of the duration of the mixing. Results for 10 min mixing are found in Figs. 6 and 7. For 30 min mixing of the PS_2/PMMA

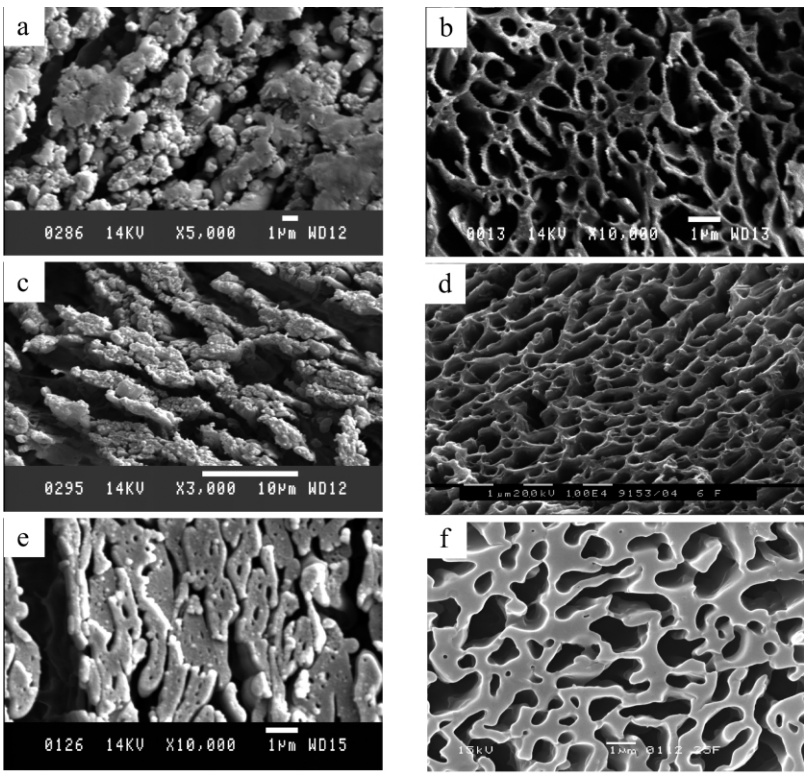

Fig. 8. SEM images of the PMMA phase after PS extraction and the PS phase after PMMA extraction in PS_2/PMMA blends for 30 min mixing: (a) and (b) $\varphi_{PMMA} = 0.50$; (c) and (d) $\varphi_{PMMA} = 0.60$; (e) and (f) $\varphi_{PMMA} = 0.70$.

blends SEM images are presented in Fig. 8 and the degree of continuity in Fig. 9. In the SEM images of Fig. 8 a BPS is observed in all three blends in the range $0.50 \leq \varphi_{PMMA} \leq 0.70$ irrespective of whether the PS_2 or PMMA phase has been extracted indicating phase co-continuity in this composition interval.

The minor phase of the $\varphi_{PMMA} = 0.40$ and the $\varphi_{PMMA} = 0.80$ samples collapsed and showed spongy type morphology after extraction of the major phase (not shown). These results indicate that $\varphi_{cr,PMMA} = 0.40 \pm 0.05$ and $\varphi_{cr,PS} = 0.20 \pm 0.05$ in PS_2/PMMA blends system. Prolonged blending times narrow the composition range in which co-continuity is observed. Determination of the critical volume fraction from Fig. 9 by extrapolation of the degree of continuity versus φ_{PMMA} curves yields $\varphi_{cr,PMMA} = 0.38$ and $\varphi_{cr,PS} = 0.20$.

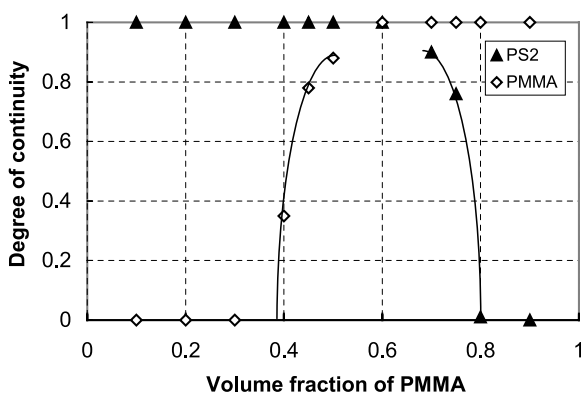

Fig. 9. Degree of continuity as a function of volume fraction of PMMA for PS_2/PMMA blends at 200 °C, 30 min mixing.

3.3. Influences of added diblock copolymer

In order to investigate how the morphology evolution is affected by an interfacial modifier, we added PS-*b*-PMMA diblock copolymer ($\varphi_{PS\text{-}b\text{-}PMMA} = 0.03$) to the PS_2/PMMA blend system. 30 min blending time was used both for blend with and without interfacial modifier. The results without interface modifier are found in Figs. 8 and 9. For the PS_2/PMMA/PS-*b*-PMMA blends SEM images are presented in Fig. 10 and the degree of continuity in Fig. 11. In the SEM images a BPS is observed in all three blends in the range $0.485 \leq \varphi_{PMMA} \leq 0.679$, $\varphi_{PS\text{-}b\text{-}PMMA} = 0.03$ irrespective of whether the PS_2 or PMMA phase has been extracted indicating phase co-continuity in this composition interval. The morphologies do not appear influenced by the presence or absence of interface modifier (compare Figs. 8 and 10) and the BPS volume fraction interval are slightly less or nearly the same with and without the addition of interface modifier within experimental error associated with the evaluation based on SEM-micrographs. Determination of the critical volume fraction from Fig. 11 by extrapolation of the degree of continuity versus φ_{PMMA} curves yields $\varphi_{cr,PMMA} = 0.44$ and $\varphi_{cr,PS} = 0.25$ indicating that the

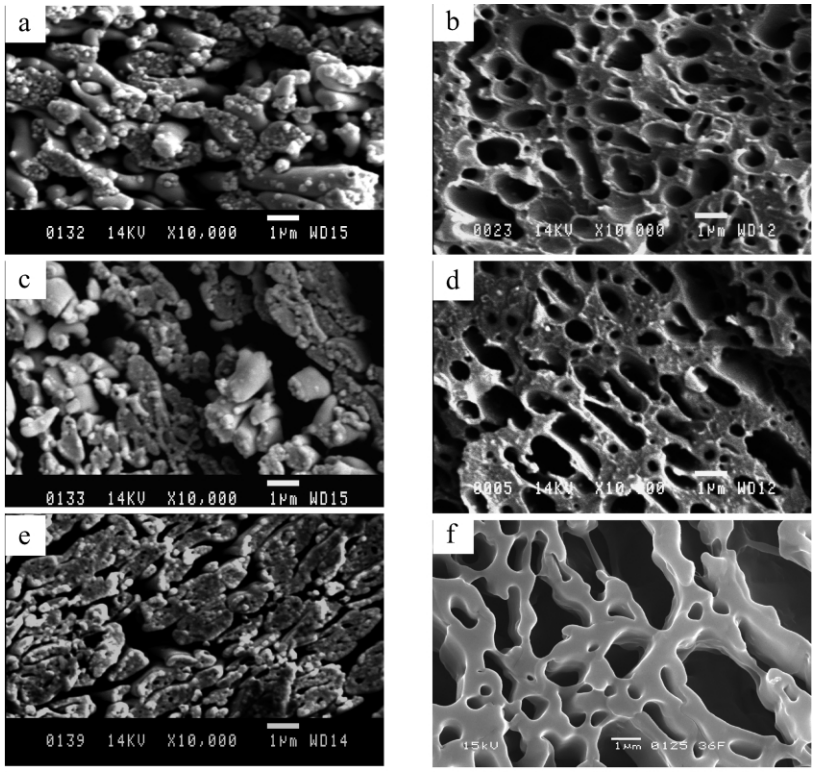

Fig. 10. SEM images of the PMMA phase after PS extraction and the PS phase after PMMA extraction in PS_2/PMMA/PS-*b*-PMMA blends at 30 min mixing: (a) and (b) $\varphi_{PMMA} = 0.485$, $\varphi_{PS\text{-}b\text{-}PMMA} = 0.03$; (c) and (d) $\varphi_{PMMA} = 0.585$, $\varphi_{PS\text{-}b\text{-}PMMA} = 0.03$; (e) and (f) $\varphi_{PMMA} = 0.679$, $\varphi_{PS\text{-}b\text{-}PMMA} = 0.03$.

addition of interface modifier causes a slight narrowing of the existence of co-continuity.

The results on the influence of composition and viscosity ratio, mixing time, and addition of interface modifier can partially be rationalized from the point of view of the principle of minimum energy dissipation in channel flow of immiscible polymers. The less viscous component will form the continuous phase and wet the channel wall where the shear stress is greatest. Thus, it is reasonable that the more viscous PMMA is prone to form the discrete phase whereas the less viscous PS is prone to form the continuous phase. In all the PS/PMMA systems investigated here $\varphi_{cr,PS} <$ $\varphi_{cr,PMMA}$. For example, the onset values of forming co-continuous structure after 10 min mixing in PS_1/PMMA blends are $\varphi_{cr,PS} = 0.16$ and $\varphi_{cr,PMMA} = 0.21$. The corresponding result for PS_2/PMMA blends are $\varphi_{cr,PS} = 0.17$ and $\varphi_{cr,PMMA} = 0.30$. These experimental results are in good agreement with the principle of minimum energy dissipation.

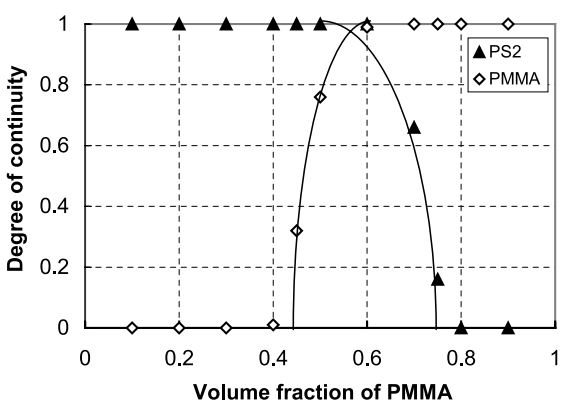

Fig. 11. Degree of continuity as a function of volume fraction of PMMA for PS_2/PMMA/PS-*b*-PMMA blends at 200 °C, 30 min mixing.

Normally, block copolymers act as surfactants to reduce blend interfacial tension and prevent coalescence leading to size reduction. However, the phenomenon is very dependent on polymer molecular weight [50]. The optimal molecular chain of block copolymer may need to be short enough to diffuse quickly to the interface but also have to be long enough to entangle sufficiently with homopolymers to prevent coalescence during blending. The block copolymer we used in this study obviously does not have the optimal molecular weight. The addition of the diblock copolymer did not significantly change the phase morphology. Much of the block copolymer might be wasted in micelles or form a separate phase rather than lie at the interface.

3.4. Morphological stability

One of the main objectives of this work was to study changes in morphology and in rheological properties of PS/PMMA blends under quiescent conditions and under shear. Therefore, it was of primary importance both to

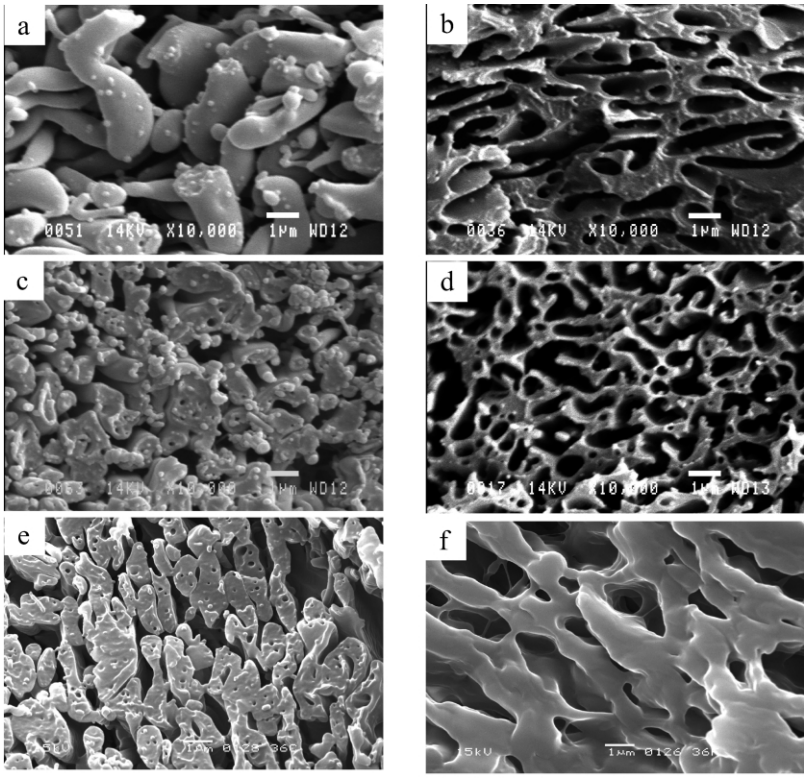

Fig. 12. SEM images of the PMMA phase after PS extraction and the PS phase after PMMA extraction in PS_2/PMMA blends for 2 min mixing: (a) and (b) $\varphi_{PMMA} = 0.40$; (c) and (d) $\varphi_{PMMA} = 0.50$; (e) and (f) $\varphi_{PMMA} = 0.70$.

identify the initial morphology and verify the stability of the initial morphology as a function of time. The PS_2/PMMA system was selected for this investigation. The mixing time was varied from 2 to 60 min. In order to better understand the behaviour under quiescent conditions, 30 min blending is compared to 2 min blending followed by annealing under quiescent conditions at the blending temperature for 28 min.

The results for 10 and 30 min blending are given in Figs. 6–9. The SEM images for 2 and 60 min mixed PS_2/PMMA blends are presented in Figs. 12 and 13, respectively. The degrees of continuity for the short and the long mixing times are given in Fig. 14. In the SEM images a BPS is observed for 2 min blending time in three blends in the range $0.40 \leq \varphi_{PMMA} \leq 0.70$ irrespective of whether the PS_2 or

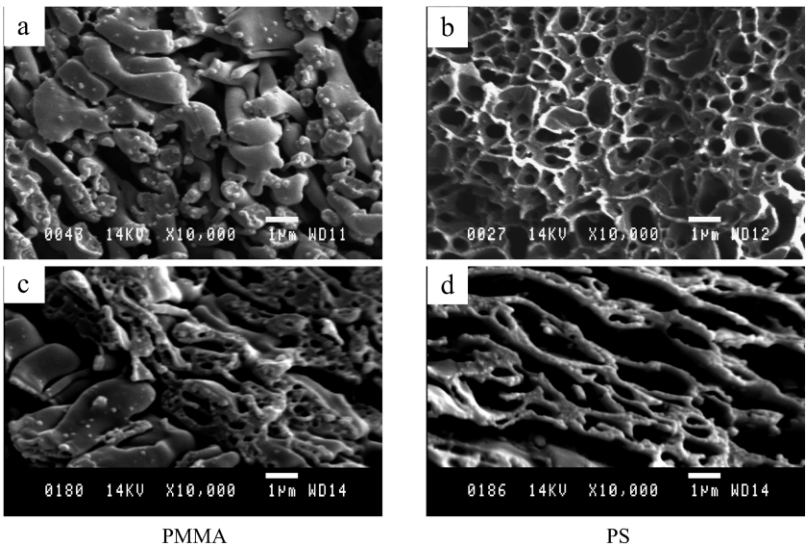

Fig. 13. SEM images of the PMMA phase after PS extraction and the PS phase after PMMA extraction in PS_2/PMMA blends for 60 min mixing: (a) and (b) $\varphi_{PMMA} = 0.50$; (c) and (d) $\varphi_{PMMA} = 0.70$.

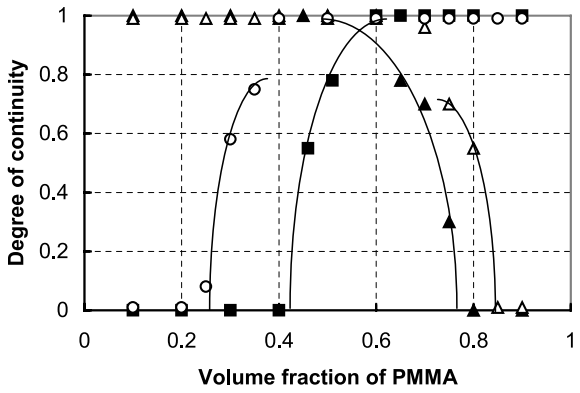

Fig. 14. Degree of continuity as a function of volume fraction of PMMA for PS_2/PMMA blends at 200 °C: (▲) PS_2, 60 min mixing; (■) PMMA, 60 min mixing; (△) PS_2, 2 min mixing; (○) PMMA, 2 min mixing.

PMMA phase has been extracted indicating phase co-continuity in this composition interval. For 60 min blending a BPS is observed for two blends in the range $0.50 \leq \varphi_{PMMA} \leq 0.70$ for both the PMMA and the PS phases. As opposed to the co-continuous $\varphi_{PMMA} = 0.40$ result after 2 min blending, the corresponding $\varphi_{PMMA} = 0.40$ after 60 min blending exhibited a PMMA powder (discrete drops) after extraction of the PS phase. This indicates that for $\varphi_{PMMA} = 0.40$ the PMMA phase is continuous after 2 min mixing whereas a discrete phase is formed after 60 min mixing. The morphology of the $\varphi_{PMMA} = 0.50$ is more or less unchanged as observed after 2 min mixing and 60 min mixing. These results indicate that after 60 min mixing $\varphi_{cr,PMMA} = 0.40 \pm 0.05$ and $\varphi_{cr,PS} = 0.20 \pm 0.05$ in PS_2/PMMA blends system whereas the corresponding values after 2 min blending are $\varphi_{cr,PMMA} < 0.30$ and $\varphi_{cr,PS} < 0.20$. Determination of the critical volume fraction from Fig. 14 by extrapolation of the degree of continuity as a function of φ_{PMMA} curves yields $\varphi_{cr,PMMA} = 0.26$ and $\varphi_{cr,PS} = 0.16$ after 2 min blending and $\varphi_{cr,PMMA} = 0.43$ and $\varphi_{cr,PS} = 0.24$ after 60 min blending.

The conclusion that was drawn based on the 10 and 30 min blending experiments is strengthened by including the 2 and 60 min blending data. Prolonged blending time narrows the composition range in which co-continuity is observed. The experimental results presented above lead us to conclude that the BPS structure formed at short mixing time in the conical twin-screw extruder ($\dot{\gamma} \approx 117$ s^{-1}) at 200 °C may be an intermediate transitional structure.

SEM images of the PMMA phase before and after 28 min annealing of the 2 min mixed samples of PS_2/PMMA blends ($\varphi_{PMMA} = 0.70$, $\varphi_{PMMA} = 0.80$, and $\varphi_{PMMA} = 0.90$) are presented in Fig. 15. The annealing of the $\varphi_{PMMA} = 0.90$ samples does not qualitatively change the well-developed dispersed morphology with a discrete PS_2 phase and a continuous PMMA phase; however, the annealing coarsened the microstructure. The $\varphi_{PMMA} = 0.70$ and $\varphi_{PMMA} = 0.80$

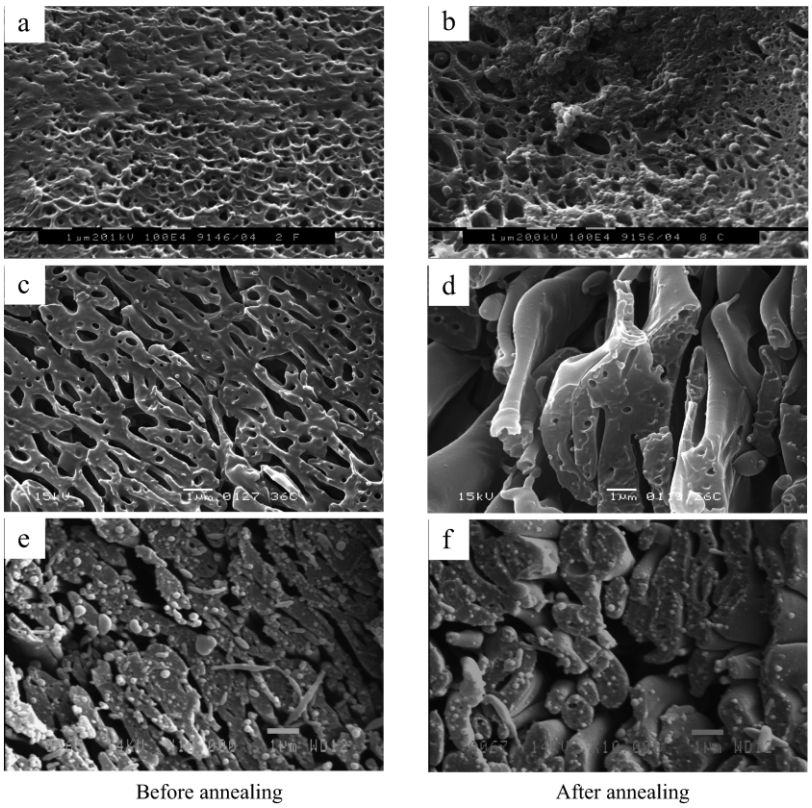

Fig. 15. SEM images of the PMMA phase after PS extraction in PS_2/PMMA blends before and after annealing at 200 °C: (a) and (b) $\varphi_{PMMA} = 0.90$; (c) and (d) $\varphi_{PMMA} = 0.80$; (e) and (f) $\varphi_{PMMA} = 0.70$.

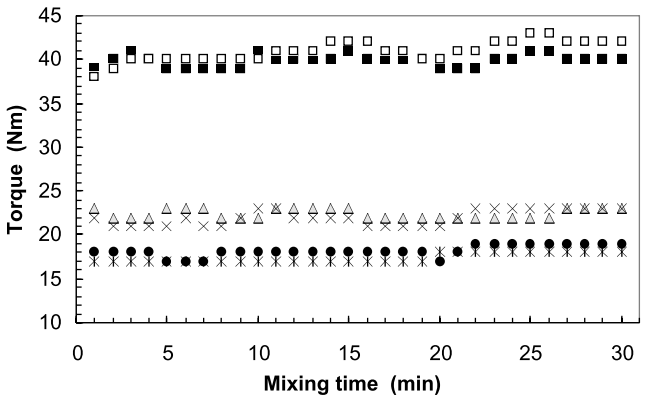

Fig. 16. Torque as a function of mixing time for PS_2/PMMA blends ($\varphi_{PMMA} = 0.80$, $\varphi_{PMMA} = 0.50$ and $\varphi_{PMMA} = 0.20$) with and without diblock copolymer: (■) $\varphi_{PMMA} = 0.80$, $\varphi_{PS\text{-}b\text{-}PMMA} = 0.00$; (□) $\varphi_{PMMA} = 0.776$, $\varphi_{PS\text{-}b\text{-}PMMA} = 0.03$; (△) $\varphi_{PMMA} = 0.50$, $\varphi_{PS\text{-}b\text{-}PMMA} = 0.00$; (×) $\varphi_{PMMA} = 0.485$, $\varphi_{PS\text{-}b\text{-}PMMA} = 0.03$; (Ж) $\varphi_{PMMA} = 0.20$, $\varphi_{PS\text{-}b\text{-}PMMA} = 0.00$; (●) $\varphi_{PMMA} = 0.194$, $\varphi_{PS\text{-}b\text{-}PMMA} = 0.03$.

samples (Fig. 15(c)–(f)) form a BPS or partial BPS (very close to co-continuity), respectively, regardless of annealing or no annealing. This means that the onset of continuity for PS_2 stays in the range $0.15 < \varphi_{cr,PS} < 0.25$ independent of annealing up to 30 min. However, the annealing experiment obviously coarsened the morphologies (Fig. 15(b), (d) and (f)).

Based on this investigation, we conclude that the co-continuous morphology type in PS_2/PMMA blends is stable at a constant temperature of 200 °C for at least 30 min in the absence of shear and that the observed changes in the blend microstructure are mainly induced by shear.

Fig. 16 shows the torque data during blending for the PS_2/PMMA blends without interface modifier ($\varphi_{PMMA} = 0.80$, $\varphi_{PMMA} = 0.50$, and $\varphi_{PMMA} = 0.20$) and the blends with interface modifier ($\varphi_{PS\text{-}b\text{-}MMA} = 0.03$; and $\varphi_{PMMA} = 0.776$, $\varphi_{PMMA} = 0.485$, or $\varphi_{PMMA} = 0.194$). Excluding a very short period at the beginning, each blend exhibits a time-independent torque and the addition of the diblock copolymer does not influence the recorded value.

3.5. Phase inversion

In this paper we have shown that BPS occurs in a rather wide volume fraction interval at mixing times of 2, 10, 30 and 60 min. No abrupt change of phase inversion has been found in PS/PMMA blends. This suggests that PS/PMMA co-continuity is qualitatively different from a phase inversion that occurs at a particular volume fraction where BPS exists. We also find that the volume fraction range in which a co-continuous structure formed becomes narrower as the mixing time is increased. Thus, we speculate that a phase inversion may occur during melt blending, and finally, shrink to one point at a sufficiently long mixing time. However, excessive melt blending may cause material decomposition.

In order to compare with theoretical predictions of phase inversion, we tentatively define the midpoint of the co-continuous region $(\varphi_{cr,PMMA} + (1 - \varphi_{cr,PS}))/2$ as the point of phase inversion. We estimate the error to be ± 0.05. Table 3 shows the torque (10 min mixing) ratios and the viscosity ratios at a shear rate of 117 s^{-1} for the PS_i/PMMA blends and the corresponding theoretical points of phase inversion calculated with Eqs. (1) and (2), respectively. The values for the point of phase inversion as calculated with the viscosity ratio (Eq. (2)) differ substantially from those based on the torque ratio (Eq. (1)). Therefore, the viscosity ratio cannot be directly correlated with the torque ratio, since the shear history inside the capillary extrusion rheometer and inside the Haake twin-screw extruder is different.

Table 3 also shows the values of the points of phase inversion predicted by Eqs. (4) and (5) in PS_i/PMMA. None of Eqs. (1), (2), (4), and (5) can predict the behaviour of both PS/PMMA blends systems studied here if the viscosity ratio is calculated at constant shear rate. Eq. (1) does a fair job for PS_1/PMMA whereas Eq. (4) works for PS_2/PMMA. Eq. (5) overestimates the phase inversion point by approximately 0.1 volumes for both blends.

However, Eq. (5) is only valid at constant stress. The viscosity ratio evaluated at constant stress for the pure component varies dramatically with stress. Since a stress profile in the twin-screw extruder is unknown, this test could not be performed in a meaningful manner. It can be seen from Fig. 2 that the viscosity ratio changes very little in the shear rate interval ($40 < \dot{\gamma} < 2000$), thus all blends should in principle be evaluated at constant stress. It is fair to conclude that the theoretical understanding of dual-phase continuity or phase inversion during the processing of immiscible binary blends is far from complete.

4. Conclusion

In this study, BPS has been evaluated by selective extraction of both phases. The critical volume fraction

Table 3
Torque and viscosity ratios, theoretical and experimental phase inversion points (φ_{PMMA}) for PS/PMMA blends at 200 °C for 10 min mixing

Sample code	T_{PS}/T_{PMMA} at 30 rpm, 200 °C	Eq. (1)	η_{PS}/η_{PMMA}, $\dot{\gamma} = 117\ s^{-1}$	Eq. (2)	Eq. (4)	Eq. (5)	Expt. phase inversion point[a]
PS_1/PMMA	0.76	0.57	0.29	0.78	0.74	0.63	0.48–0.58
PS_2/PMMA	0.40	0.71	0.15	0.87	0.61	0.68	0.54–0.64

Torque is measured at DTU laboratory using Haake MiniLab Rheomex CTW5 twin-screw extruder for 10 min mixing.
[a] Taken from the midpoint of the co-continuous region of ±0.05 volume fraction and the degree of continuity (see text).

evaluated by observation of forming stability of samples after extraction of the major phase (direct observation) corresponds well with the estimate obtained from extrapolation of continuity index estimated by extraction of the minor phase.

The results show that the most significant factors determining the onset of co-continuous structure during melt blending in PS/PMMA blends are blend composition and viscosity ratio. It is found that dual-phase continuity occurs in a wide composition range at short mixing times. Increasing mixing time and addition of diblock copolymer lead to narrowing of the composition range in which dual-phase continuity exists. It is also found that a co-continuous structure may not be stable and may be transformed into a dispersed structure after sufficient mixing times. The qualitative features of the observed morphologies are unaffected by quiescent annealing up to 30 min, but coarsening was observed.

Phase inversion predictions of semi-empirical models have been compared with experimental results obtained from PS/PMMA blends. None of these models are successful in predicting the observed behaviour.

Acknowledgements

The financial support of the Technical Science Council of Denmark is gratefully acknowledged. The authors would like to thank Professor David Plackett for his help in reviewing this manuscript.

References

[1] Lyngaae-Jørgensen J, Lunde Rasmussen K, Chtcherbakova EA, Utracki LA. Polym Engng Sci 1999;39:1060.
[2] Grace HP. Chem Engng Commun 1982;14:255.
[3] Elmendorp JJ, Maalcke RJ. Polym Engng Sci, Part 1 1985;25:1041.
[4] Favis BD. Can J Chem Engng 1991;69:619.
[5] Utracki LA, Shi ZH. Polym Engng Sci 1992;32:1824.
[6] Favis BD, Chalifoux JP. Polym Engng Sci 1987;27:1591.
[7] Scott CE, Macosko CW. Polym Bull 1991;26:341.
[8] Lyngaae-Jørgensen J, Utracki LA. Makromol Chem, Macromol Symp 1991;48/49:185.
[9] Scott CE, Macosko CW. Polymer 1995;36:461.
[10] Mekhilef N, Verhoogt H. Polymer 1995;37:4069.
[11] Cartier H, Hu GH. Polym Engng Sci 1999;39:996.
[12] Lee JK, Han CD. Polymer 1999;40:2521.
[13] Lee JK, Han CD. Polymer 2000;41:1799.
[14] Martin P, Carreau PJ, Favis BD. J Rheol 2000;44:569.
[15] Chuai CZ, Almdal K, Johannsen I, Lyngaae-Jørgensen J. Polymer 2001;42:8217.
[16] Lazo NDB, Scott CE. Polymer 2001;42:4219.
[17] Shih CK. SPE ANTEC 1991;37:99.
[18] Ratnagiri R, Scott CE. Polym Engng Sci 1999;39(9):1823.
[19] Scott CE, Joung SK. Polym Engng Sci 1996;36(12):1666.
[20] Shih CK. Adv Polm Technol 1992;11(3):223.
[21] Sundararaj U. Macromol Symp 1996;112:85.
[22] Shih CK. Polym Engng Sci 1995;35(21):1688.
[23] Lazo NDB, Scott CE. Polymer 1999;40(20):5469.
[24] Ratnagiri R, Scott CE, Shih CK. Polym Engng Sci 2001;41:1019.
[25] Fortelny I, Zivny A. Polymer 1995;36(21):4113.
[26] Park I, Barlow JW, Paul DR. J Polym Sci, Part B: Polym Phys 1992; 30(9):1021.
[27] Scott CE, Macosko CW. Polym Engng Sci 1995;35(24):1938.
[28] Willemse RC, Ramaker EJJ, Van Dam J, De Boer AP. Polym Engng Sci 1999;39(9):1717.
[29] Jordhamo GM, Manson JA, Sperling LH. Polym Engng Sci 1986;26: 517.
[30] Paul DR, Barlow J. J Macromol Sci, Rev Macromol Chem (C) 1980; 18:109.
[31] Miles IS, Zurek A. Polym Engng Sci 1988;28:796.
[32] Avgeropoulos GN, Weissert FC, Biddison PH, Bohm GGA. Rubber Chem Technol 1976;49:93.
[33] Harrats C, Blacher S, Fayt R, Jerome R, Teyssie P. J Polym Sci, Part 3: Polym Phys 1995;33:801.
[34] Levij M, Maurer FH. J Polym Engng Sci 1988;28:670.
[35] Metelkin VI, Blekht VS. Colloid J USSR 1984;46:425.
[36] Utracki LA. J Rheol 1991;35:1615.
[37] Stauffer D. Introduction to percolation theory. London: Taylor & Francis; 1985.
[38] Paul DR, Newman S, Polymer blends, vols. 1/2. New York: Academic Press; 1978.
[39] Xanthos M. Reactive extrusion. New York: Hanser; 1992.
[40] Lyngaae-Jørgensen L. Int Polym Proc 1999;14:213.
[41] Utracki LA. Polymer alloys and blends. New York: Hanser; 1989.
[42] Danesi S, Porter RS. Polymer 1978;19:448.
[43] Nelson CJ, Avgeropoulos GN, Weissert FC, Bohm GGA. Angew Makromol Chem 1977;60/61:49.
[44] Renfree RW, Nosker TJ, Morrow DR, Van Ness KE, Wyatt ED, Suttner LW. SPE Tech Papers 1992;50:2396.
[45] Hsu WY, Wu S. Polym Engng Sci 1993;33:293.
[46] Arends CB. Polym Engng Sci 1992;32:841.
[47] Chuai CZ, Almdal K, Johannsen I, Lyngaae-Jørgensen J. J Mater Sci Lett 2002;21:89.
[48] Quintens D, Groeninckx G, Guest M, Aerts L. Polym Engng Sci 1990; 30:1484.
[49] Andradi LN, Hellmann GP. Polym Engng Sci 1995;35:693.
[50] Macosko CW, Guegan P, Khandpur AK, Nakayama A, Marechal P, Inoue T. Macromolecules 1996;29:5590.
[51] Orwoll RA. Physical properties of polymers handbook. Woodbury: American Institute of Physics; 1996.